Reduction of Iron Oxide Catalysts: The Investigation of Kinetic Parameters Using Rate Perturbation and Linear Heating Thermoanalytical Techniques

Michael. J. Tiernan,† Philip. A. Barnes,* and Gareth. M. B. Parkes

Centre for Applied Catalysis, Materials Research Division, University of Huddersfield, Queensgate, HD1 3DH, U.K.

Received: September 5, 2000; In Final Form: November 1, 2000

The mechanisms and kinetics of the reduction of powdered Fe_2O_3 and Fe_3O_4 samples have been investigated under nonisothermal conditions to provide a detailed insight into the processes occurring. Both conventional linear heating temperature-programmed reduction (TPR) and constant rate temperature-programmed reduction (CR-TPR) techniques were utilized. Fe_2O_3 was found to reduce to Fe in a two-step process via Fe_3O_4. The mechanism of the prereduction step of Fe_2O_3 to Fe_3O_4 was found to follow an *n*th order expression where nucleation or diffusion was not the rate-controlling factor while the main reduction step to metal was described by a model involving the random formation and growth of nuclei. A CR-TPR rate perturbation method, "rate-jump", was applied to the measurement of variations in apparent activation energy throughout the reduction processes, under near-equilibrium conditions and the activation energy measurements are compared with those obtained under conventional linear heating conditions.

1. Introduction

1.1. Reduction of Iron Oxide. The reduction of iron oxides by both hydrogen and carbon monoxide has been investigated very extensively because of its relevance for iron production and the preparation of ammonia synthesis catalysts.[1,2−11] Iron has three oxides, namely hematite (Fe_2O_3), magnetite (Fe_3O_4), and wüstite (FeO). The latter is unstable below 570 °C when it decomposes to α-Fe and Fe_3O_4.[9] The literature suggests that the reduction of Fe_2O_3 to Fe metal, at temperatures below 570 °C, proceeds in two steps via Fe_3O_4 intermediate as follows:

$$3Fe_2O_3 + H_2 \rightarrow 2Fe_3O_4 + H_2O \quad \text{Step 1}$$

$$Fe_3O_4 + 4H_2 \rightarrow 3Fe + 4H_2O \quad \text{Step 2}$$

Step 1 is exothermic, while reduction to the metal in step 2 is endothermic.[3] Discrepancies exist in the kinetic model(s) which have been reported for the reduction steps. Such inconsistencies may be attributed to variations in the type of sample specimen used (powder, pellet, or ore) and the experimental conditions employed (temperature, pressure, isothermal, nonisothermal).[1,2,8] In particular, differences are found in the literature in the conditions of reduction temperature, H_2O pressure, and particle/crystallite size. Comparisons are further complicated because not only do different oxides exist but also the presence of impurities (e.g., Ca, Mn, and Mg in ores)[8] and dopant materials (e.g., K in ammonia synthesis catalysts)[11] may significantly affect the reduction process.[2,3] In the case of reduction of either hematite or magnetite at temperatures above 600 °C, the formation of a stable wüstite phase must also be considered.[10]

1.2. Kinetic Studies of Iron Oxide Reduction. Kinetic data for the reduction of metal oxides are generally interpreted in terms of nucleation, auto-catalytic, or contracting sphere (phase boundary) models of reduction (discussed in detail below).[12] The reductions of Fe_2O_3 and Fe_3O_4 to Fe have been reported to follow all of these models, with variations attributed to experimental factors such as sample particle size or the conditions chosen for analysis.[1,2,5,8] Larger particle sizes have been reported to reduce via a phase boundary mechanism (topochemical mode of reaction) while smaller particles tend to show sigmoidal reduction isotherms associated with a formation and growth of nuclei model (uniform internal reduction) particularly at lower temperatures.[1] An auto-catalytic role of freshly formed Fe particles in the presence of certain levels of water vapor (2−7.5 v/v% in the reducing mixture) has also been proposed involving transport of active hydrogen from metal sites to the oxide through "portholes" of water vapor trapped between the metal and oxide phases.[3,4] However, in general the addition of H_2O is reported to retard the reduction rate particularly for the $Fe_3O_4 \rightarrow Fe$ step.[1]

Conventionally, reduction kinetics of metal oxides, such as Fe_2O_3 or Fe_3O_4, have been studied under isothermal conditions where the extent of reduction, α, is measured as a function of time. In recent years, nonisothermal techniques for the investigation of kinetic parameters have become popular because of their less cumbersome and tedious nature when compared with a series of isothermal experiments at different temperatures.[13] In particular, temperature-programmed reduction (TPR) experiments have been performed using linear heating rates to investigate the reduction of metal oxides and metal salts as a function of temperature. The inherent simplicity and high sensitivity of linear heating TPR make it a very important analytical method which has provided extremely valuable information in a range of areas including the characterization and preparation of catalysts.[12] Unfortunately, the use of linear heating rates in thermal analysis techniques results in nonuniform reaction conditions throughout the sample leading to relatively poor resolution and kinetic data.[14−16] Further difficulties arise in TPR, because variations in sample mass, heating rate or gas flow rate lead to different H_2 consumption rates.

* Corresponding author. E-mail: p.a.barnes2@hud.ac.uk.
† Current address: School of Chemical Sciences, Dublin City University, Dublin 9, Ireland

10.1021/jp003189+ CCC: $20.00
Published on Web 12/13/2000

For these reasons, TPR profiles are known to be remarkably dependent on the experimental conditions employed which can affect both the shape and resolution of reduction steps as well as peak temperatures.[12,14,15−17]

Such limitations of linear heating TPR can be illustrated by examples of the reduction of Fe_2O_3 taken from the literature. Satisfactory resolution of the two steps involved in the reduction of Fe_2O_3 has been found to be difficult to achieve under linear heating rate TPR conditions.[1] Combined with a lack of sensitivity, this can limit ability to gain a detailed insight into step 1 of the hematite reduction process.[1] Prudent choice of experimental conditions, such as H_2 and H_2O pressure, is also essential. The level of H_2O in the reducing mixture has been shown to affect both the rate and the mechanism of reduction.[1,3,4] The H_2 partial pressure employed has also been shown to affect both peak temperatures and resolution.[6,16] Comparison of previous literature studies using unsupported iron oxides has shown that the use of integral conditions with respect to H_2 and H_2O pressures may result in strongly deformed and broadened peaks when compared with profiles obtained under differential conditions, emphasising the care required when performing linear heating rate experiments.[1,2]

To provide more optimal conditions for kinetic analysis of TPR profiles we have recently described an apparatus developed to perform reduction under constant rate thermal analysis (CRTA) conditions as well as conventional linear heating rates.[18] The advantages of CRTA, where the reaction is forced to proceed at a low and constant rate, are well documented for the study of decomposition and reduction reactions.[18−21] In comparison with linear heating rate methods, CRTA reduces temperature and pressure gradients across the sample bed and allows reactant and product gases to be maintained at a constant concentration level. In this manner, CRTA provides superior control of mass and thermal transfer effects while application of a "rate-jump" method allows the apparent activation energy of reaction to be determined under near-equilibrium conditions.[18,22] CR-TPR can also provide enhanced resolution for overlapping reduction events while the shape of the temperature profile obtained gives an insight into reduction mechanisms of supported and unsupported samples.[18]

In the present study, CR-TPR is used to investigate kinetic aspects of the reduction of iron oxides (hematite and magnetite) under experimental conditions designed to optimize resolution of the reduction events and provide a mechanistic insight into each event. Results are compared to those obtained under linear heating conditions.

2. Theory

2.1. Kinetic Model. Gas−solid reactions such as reductions are typified by complex kinetics which frequently cannot be described by a single nth-order expression over the entire reaction range.[1,18] Kinetic interpretation of thermal analysis data is normally carried out using equations based on the general kinetic equation:

$$\text{rate} = d\alpha/dt = A\, f(\alpha)\, \exp^{-E/RT} \qquad (1)$$

where A is the preexponential factor, T is the absolute temperature, t is the time, α is the fraction of sample reacted, E is the activation energy, R is the gas constant (8.314 J mol^{-1} K^{-1}), and $f(\alpha)$ is a function which represents the reaction mechanism. The aim is to determine the kinetic model ($f(\alpha)$) which gives the best description of the studied reaction and allows the calculation of meaningful parameters E and A.

The most frequently cited kinetic models can be categorized into three groups which describe diffusion-controlled processes, boundary-controlled (nth-order processes), and processes involving random nucleation and subsequent growth of nuclei.[1,23−25] Algebraic expressions ($f(\alpha)$) for each of these models can be found in the literature.[1,22,23] For diffusion-controlled processes, gas diffusion through the product layer is the rate-determining step. Phase boundary-controlled models are geometrically defined as shrinking/unreacted core or contracting sphere models with the reaction proceeding topochemically and in which the chemical reaction is the rate-determining step. In terms of the reduction of metal oxides, nucleation-controlled processes involve uniform internal reduction and occur by the initial random removal of lattice oxygen atoms until a critical concentration of vacancies is reached. The vacancies are then annihilated by lattice rearrangement to produce metal nuclei. The nuclei then grow and, as they expand, the reduction process accelerates due to the increasing metal−metal oxide interface which is further increased by the formation of new nuclei. Eventually, merging of product nuclei causes a decrease in sample−product interfacial area and the reduction decelerates. Autocatalytic mechanisms, where the product metal dissociates hydrogen molecules thereby increasing the rate of reduction of remaining metal oxide, must also be considered when studying solid−gas reductions.[1,12]

It is well-known that a number of experimental factors, such as geometric considerations, are important in solid-state reactions and can produce significant deviations in $f(\alpha)$ and the measured values of A and E for a given reaction.[27] In such circumstances, it is not appropriate to interpret E in terms of the usual energy barrier model of homogeneous chemical reaction kinetics and, for this reason, the term apparent activation energy is often applied.[22]

2.2. Apparent Activation Energy Measurements. Kinetic analysis of linear heating rate and CRTA "rate-jump" experiments can be achieved using methods based on the general kinetic eq 1 above. The methods used in the current study are outlined below.

2.2.1. Linear Heating Rate Methods. Wimmers et al.[1] have proposed a method, based on eq 1, which allows the apparent activation energy, E_a, for the reduction of iron oxide under linear heating conditions to be determined using the following equation:

$$\ln\left(\frac{\beta}{T_m^{\,2}}\right) = \frac{-E_a}{RT_m} + \ln\left(\frac{AR}{E_a}\right) + \text{constant} \qquad (2)$$

where β is the heating rate.

When $\ln(\beta/T_m^2)$ is plotted versus $1/T_m$ a straight line is obtained with a slope of $-E_a/R$.[1,18] No prior knowledge of the kinetic model describing the reduction mechanism is required in order to calculate E_a. This method assumes that any changes in reduction mechanism and the extent of reduction (α) at T_m, caused by changes in the heating rate employed, are negligible. Wimmers and coauthors[1] noted that eq 2 is generally applicable for the determination of activation energy from conventional TPR measurements.

2.2.2. CRTA "Rate-Jump" Method. The underlying principles and exact measurement procedures associated with the use of the CRTA "rate-jump" method for the determination of model-free activation energy values have been previously described for gas−solid reduction[18] and solid-state decomposition[22] reactions. In this technique, the rate of reaction is made to alternate between two pre-selected target rates by appropriate control of

the temperature[20] or, for certain systems, the concentration of a reactant gas.[28] In the former case, provided equilibrium of the reaction rate is achieved at the two successive rates, the corresponding temperature measurements can be used to calculate a value of E_a for the reaction using the following form of the Arrhenius equation:

$$E_a = RT_1\frac{T_2}{T_1 - T_2}\ln\left(\frac{C_1}{C_2}\right) \quad (3)$$

where T_1 and T_2 are the temperature measurements corresponding to the two pre-set reaction rates C_1 and C_2, at the same value of α (extent of reaction).[21] To ensure that T_1 and T_2 values for each jump correspond to the same extent of reaction, an extrapolation procedure is performed using best-fit curves drawn through the higher and lower levels of successive "jumps" for both temperature and reduction rate as detailed in a previous paper.[22]

The use of the "rate-jump" method to provide measurements of thermally activated reactions has been recommended since the results obtained are less dependent on experimental parameters than those obtained with conventional techniques[21,26,29] as the effects of heat and mass transfer can be minimized.[20] This can be most successfully achieved if the target reduction rates, C_1 and C_2, as well as the difference between the selected rates, be maintained as low as possible in order to minimize heat and mass transfer effects throughout the reduction process as well as changes in reactant and/or product concentration during each jump. The method assumes that any changes in $f(\alpha)$, as well as α, during each "rate-jump" are negligible, emphasising the requirement that the execution time for each jump be small in comparison with the duration of the reaction. Furthermore, by making a large number of "rate-jump" measurements, any variation in E_a throughout the reaction can be quantified.[18,22]

The use of low overall reaction rates ensures that near-equilibrium conditions are reached. While each experiment may therefore last for many hours there is no need for the series of runs at different temperatures (for isothermal work) or at various heating rates (for linear heating experiments). Not only does this save time but it also removes uncertainties which can arise in a series of experiments due to the inevitable slight variations in the sample and experimental conditions.

It should be noted that in the CRTA "rate-jump" method, the resolution of two consecutive events is often more clearly seen from the temperature curve.[18] In an ideal experiment, the reaction rate curve would show no discontinuity between two such processes which would be revealed only by reference to the temperature trace.

3. Experimental Section

3.1. Materials. Fe_2O_3 (99.98%, Aldrich) and Fe_3O_4 (99.997%, Alfa Chemicals) were used. Samples were sieved through a 250 μm mesh prior to all experiments.

3.2. Materials Characterization. X-ray diffraction (XRD) spectra of Fe_2O_3 and Fe_3O_4 samples were obtained using Cu Kα ($\lambda = 1.5418$ Å) radiation. Scanning electron micrography (SEM) images were obtained using a S-3000N Hitachi instrument. The surface area of each sample was estimated using the BET method based on the adsorption of N_2 at -195 °C using a Micromeritics Gemini Analyzer instrument and pore size analysis was performed using a Coulter SA 3100 instrument.

3.3. TPR Conditions. The TPR apparatus, which uses a hygrometer to detect H_2O evolved during reduction, has been described previously.[18] Important features of the apparatus include direct sample temperature measurement, a fast response furnace, and a highly sensitive specific detector. Rapid computer control of the furnace heating or cooling rates allows regulation of the reaction rate, at pre-set values, via a feedback loop for CRTA experiments.

For all experiments the reduction atmosphere consisted of 5% hydrogen in helium at a flow rate of 52 cm^3 min^{-1}. Conventional TPR experiments were performed using a variety of linear heating rates in the range of 2 to 15 °C min^{-1}. Equation 2 was then used to yield values for the apparent activation energy of the reduction. A sample mass of 2.0 ± 0.1 mg was employed in all linear heating rate experiments.

Details of the experimental conditions employed for CRTA "rate-jump" experiments are shown in Table 1. Experiments were performed using maximum heating and cooling rates of 5 and 10 °C min^{-1}, respectively. The heating rate was varied between these two limits in order to alternate between two pre-selected target reduction rates, C_1 and C_2. Equation 3 was then used to calculate the activation energy for each jump.

TABLE 1: Experimental Conditions Employed for CRTA "Rate-Jump" Experiments for the Reduction of Fe_2O_3 and Fe_3O_4 Samples

sample	sample mass (mg)	C_1[a] (mg H_2O min^{-1})	C_2[b] (mg H_2O min^{-1})	no. of "rate-jumps"
Fe_2O_3	30.0	3.6×10^{-3}	4.4×10^{-3}	132
Fe_3O_4	30.0	3.6×10^{-3}	4.4×10^{-3}	116

[a] C_1 = lower water evolution rate target. [b] C_2 = higher water evolution rate target.

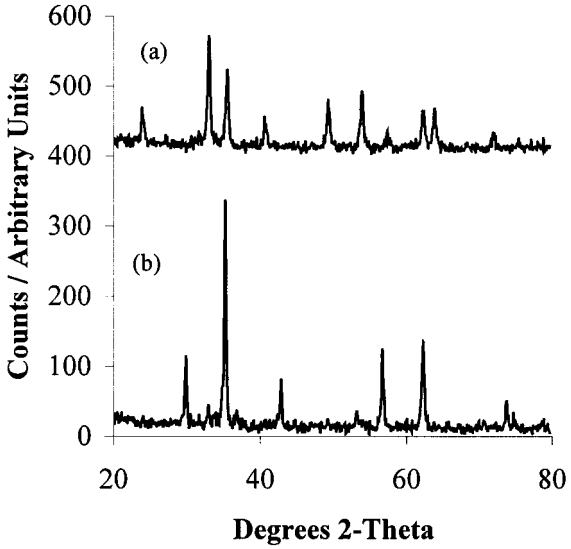

Figure 1. X-ray diffraction powder patterns of Fe_2O_3 (a) and Fe_3O_4 (b) samples.

4. Results and Discussion

4.1. Materials Characterization. XRD patterns are shown in Figure 1 which confirm the structure of Fe_2O_3 and Fe_3O_4 samples with the main peak for Fe_2O_3 present at a 2θ angle of 33.0° (Figure 1a) and for Fe_3O_4 at 2θ angle of 35.2° (Figure 1b).[3,30] Representative SEM images of the two samples are shown in Figure 2 at low (Figure 2b,d) and high (Figure 2a,c) magnification. The Fe_2O_3 sample (Figure 2a,b) consists of chipped particles of various shapes with flat sharp-edged surfaces. By contrast, the Fe_3O_4 sample (Figure 2c,d) is seen to consist of much smaller particles with a more lustrous and less

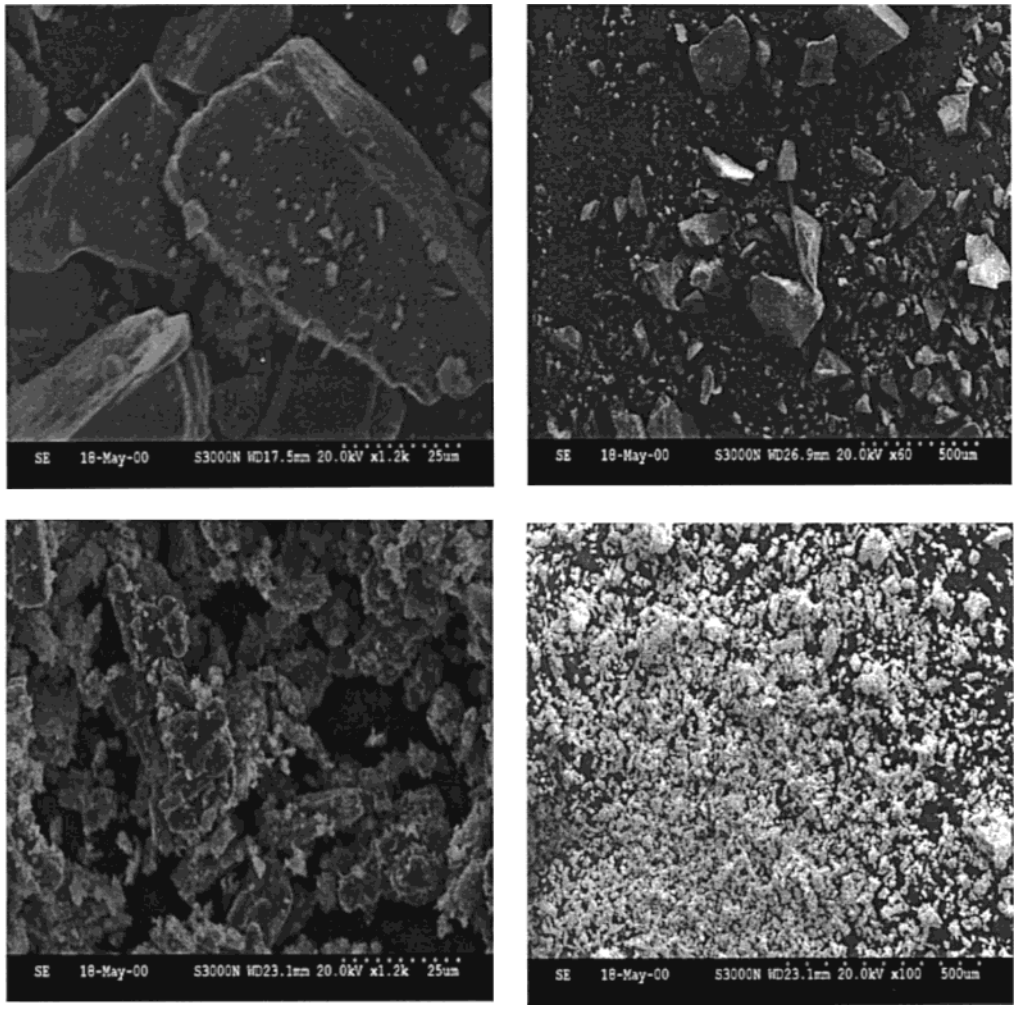

Figure 2. Typical SEM photographs of Fe_2O_3 (a,b) and Fe_3O_4 (c,d) samples.

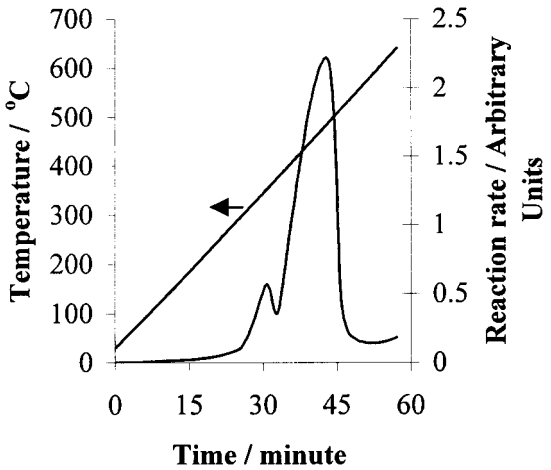

Figure 3. TPR profile of Fe_2O_3 under linear heating rate conditions.

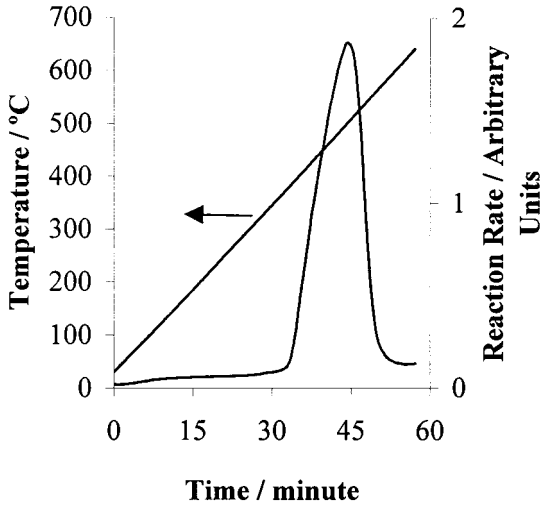

Figure 4. TPR profile of Fe_3O_4 under linear heating rate conditions.

defined surface. BET surface areas of 160 $m^2\ g^{-1}$ and 2 $m^2\ g^{-1}$ and total pore volumes of 0.185 $cm^3\ g^{-1}$ and 0.005 $cm^3\ g^{-1}$ were measured for Fe_2O_3 and Fe_3O_4, respectively.

4.2. Comparison of CRTA and Linear Heating Techniques. Figures3 and 4 illustrate TPR results obtained under linear heating conditions for the Fe_2O_3 and Fe_3O_4 samples. Figure 3 shows a typical TPR profile for Fe_2O_3 obtained using a linear heating rate of 10 °C min^{-1}. The maximum rate of H_2O production was ca. 4.35×10^{-2} mg min^{-1} for the major peak. Under all linear heating rates employed the reduction of Fe_2O_3 showed two overlapping peaks indicating a two-step reduction process. Depending on the heating rate employed, the peak maximum ranged from 327 to 383 °C for the minor peak and from 389 to 522 °C for the major peak (see Table 2). Shimokawabe et al.[2] reported peak temperatures of 350 °C and 550 °C in the TPR profile of an Fe_2O_3 sample prepared by decomposition of $Fe(OH)(CH_3COO)_2$ in air at 500 °C and reduced under a linear heating rate of 4.5 °C min^{-1}. Meaningful comparison of exact peak temperatures with other studies is

TABLE 2: Variation of T_m with Linear Heating Rate (β) for Fe_2O_3 Reduction

β (°C min^{-1})	T_m (°C) peak [1]	T_m (°C) peak [2]
2	327	389
5	353	438
10	373	491
15	383	522

TABLE 3: Variation of T_m with Linear Heating Rate (β) for Fe_3O_4 Reduction

β (°C min^{-1})	T_m (°C)
2	410
5	458
10	503
15	531

difficult because of the different experimental and pretreatment conditions employed by the various workers.[12] However, most literature agrees that the reduction of powdered hematite to metallic iron involves two stages via the formation of magnetite (steps 1 and 2, discussed above).[1−3] Boot et al.[6] reported only one unresolved reduction peak for Fe_2O_3 in a physical mixture (3 wt % Fe) with ZrO_2. However, this could be attributable to the high concentration of H_2 (70% in Ar) employed for linear heating TPR which would be expected to result in poor resolution of overlapping events.

Figure 4 shows the TPR profile obtained for Fe_3O_4 under linear heating conditions of 10 °C min^{-1}. A single peak is observed over a temperature range of ca. 370−610 °C with a maximum at 502 °C. The maximum rate of H_2O production is ca. 3.69×10^{-2} mg min^{-1}. Peak temperatures at other heating rates employed are shown in Table 3. Comparison of Tables 2 and 3 shows that at all heating rates employed the peak temperature for $Fe_3O_4 \rightarrow Fe$ reduction was higher during reduction of Fe_3O_4 starting material relative to the peak temperature for the second step in the reduction of Fe_2O_3 sample. Differences in reducibility might be associated with the higher surface area of the Fe_2O_3 sample providing a greater number of reactive sites at which reduction can start.[2,31]

Figure 5 shows the reduction profile of Fe_2O_3 under CRTA "rate-jump" conditions. The reduction takes place in two consecutive steps as can be seen by the discontinuity in the temperature curve. The temperature profile shows how the computer control system attempts to alternate between the preset reaction rates throughout each step. The target reaction rates were maintained over a temperature range of 250−270 °C for the first reduction step while the majority of the second step occurs at the pre-selected rates over the temperature range of 245−295 °C. This shows that the reduction steps can be achieved at a much lower temperature than indicated in Figure 3 under conventional linear heating conditions. It also shows that a large proportion of the second step in the reduction occurred within the same temperature range as the first temperature step even though the steps are consecutive in occurrence. This is associated with a difference in the mechanism of the two steps which is not apparent from linear heating rate profiles and is discussed in more detail below.

Figure 6 shows the CRTA "rate-jump" profile obtained for the reduction of Fe_3O_4. The reduction is seen to proceed in a single step across a temperature range of 260−345 °C, as judged by a lack of discontinuity in the temperature trace.

4.3. Mechanism and Apparent Activation Energy of Reduction. Figure 7 shows the α versus temperature profile for the linear heating rate experiment (Figure 7a) and the CRTA "rate-jump" experiment (Figure 7b) for the reduction of Fe_2O_3, the latter form of presentation being valuable for quantitative comparisons. From both curves, it is seen that the first reduction step accounts for approximately 11% of the overall reduction process. A value of 11.1% corresponds to the formation of Fe_3O_4, with 88.9% of the H_2O production associated with subsequent reduction to Fe. It is apparent from Figure 7 that the resolution of the two events is greater under CRTA conditions than using conventional linear heating with the α profile in Figure 7b confirming that the prereduction step to Fe_3O_4 is complete prior to the onset of the main reduction step to metallic iron. This agrees with previous literature studies on powder Fe_2O_3 samples which generally report that the reduction proceeds in two consecutive steps.[1,2,3] Sastri and co-workers[3] reported that findings from X-ray diffractometry, Mössbauer spectroscopy and photomicrography studies showed that the reduction proceeds in a stepwise manner with only two phases, either Fe_2O_3 and Fe_3O_4 or Fe_3O_4 and Fe, existing at any stage throughout isothermal reduction below 570 °C. Jung and Thompson[5] showed using a dynamic X-ray diffraction (DXRD) technique that the isothermal reduction of Al_2O_3-supported Fe_2O_3 (31.8 wt % Fe) to Fe at 400 °C proceeded via Fe_3O_4 and that it was only after complete reduction of hematite to magnetite

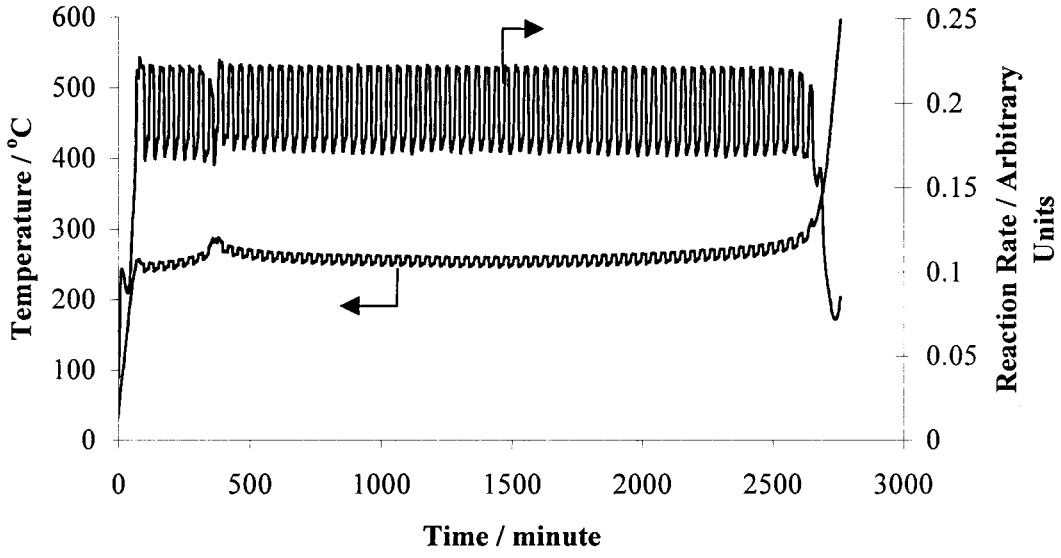

Figure 5. TPR profile of Fe_2O_3 under CRTA "rate-jump" conditions.

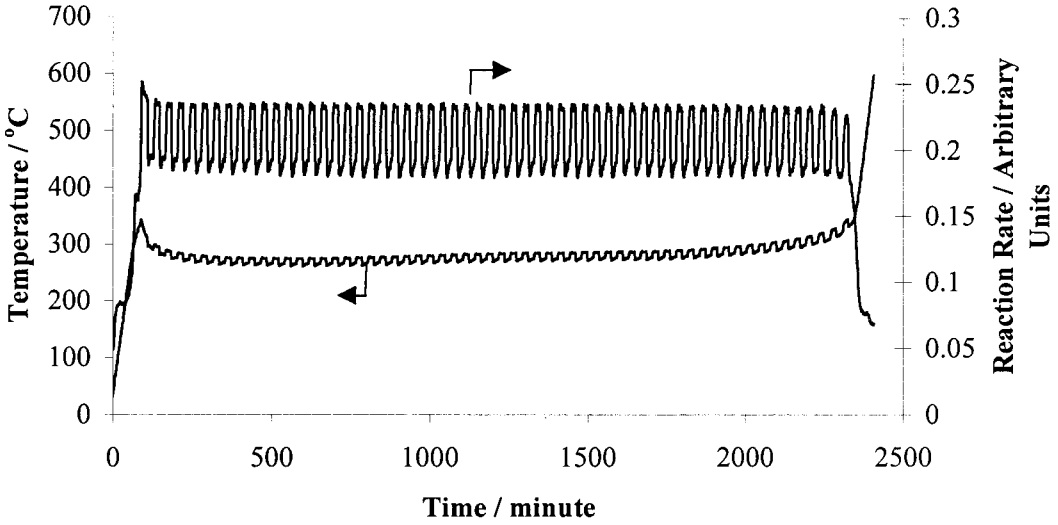

Figure 6. TPR profile of Fe_3O_4 under CRTA "rate-jump" conditions.

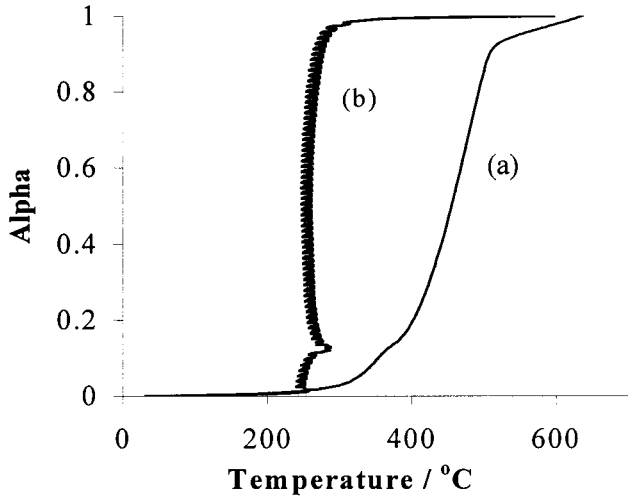

Figure 7. Extent of reaction (α) versus temperature plot for the TPR of Fe_2O_3 under (a) linear heating and (b) CRTA '"rate-jump" conditions.

that the latter was then further reduced to iron. Shimokawabe et al.[2] also reported that the reduction of α-Fe_2O_3 samples, prepared by decomposition of iron salts at temperatures below 700 °C, proceeded via a two-step mechanism with the Fe_2O_3 → Fe_3O_4 step being completed before the onset of the Fe_3O_4 → Fe step under linear heating rate conditions of 4.5 °C min^{-1}. However, for samples prepared by decomposition of salts at temperatures above 900 °C, steps 1 and 2 occurred simultaneously under the reduction conditions employed.[2] Wimmers et al.[1] reported that the Fe_2O_3 → Fe_3O_4 step was either advanced significantly or completed before onset of the Fe_3O_4 → Fe reduction step in linear heating rate experiments under various conditions. Discrepancies were attributed to variations in the samples of Fe_2O_3 as well as the experimental conditions employed. In the present study, the CRTA profile in Figure 7b shows that if the reduction is forced to proceed at a slow rate then the prereduction to Fe_3O_4 is completed prior to subsequent reduction to Fe.

The shape of α versus temperature profiles in CRTA experiments can reveal information on the mechanism of solid-state reactions.[18,22,24] The form of the α profile for the main reduction step in Figure 7b indicates that the Fe_3O_4 → Fe reduction follows a nucleation or autocatalytic mechanism (discussed above) with a rise, fall, and then rise again in temperature required to maintain a constant reaction rate throughout the reduction step. This causes the α versus temperature profile to characteristically curve back on itself during the reduction process.[18,24,31] This can be explained as follows. The temperature increases at first until the initial formation of nuclei after which the temperature decreases in order to maintain a constant reduction rate as the metal−metal oxide interfacial area expands. Toward the later stages of reduction, the expanding nuclei start to overlap and the area of the sample-product interface starts to decrease so the temperature has to rise again to prevent deceleration of the reaction. In some cases, metal nuclei formed are believed to dissociate and activate dihydrogen molecules leading to autocatalysis which could also result in a similar α versus temperature profile to that obtained for the main reduction step in Figure 7b. The shape of the α versus temperature plot obtained for the prereduction step of Fe_2O_3 indicates that a different kinetic model was in operation for this step as a continual rise in temperature was required to maintain the desired reduction rate. This profile shape is associated with an "*n*th-order" type of kinetic model where nucleation or diffusion are not the rate-controlling factors.[22,24] Although the second step is initiated at a higher temperature than the prereduction step it can be seen from Figure 7b that a large proportion of the main reduction step proceeded within the same temperature range as the prereduction to Fe_3O_4 under CRTA experiments. Although the initial formation of nuclei in the reduction of Fe_3O_4 requires a higher temperature than is required for the prereduction step, once the nuclei formed begin to grow the reaction accelerates and a lower temperature is then capable of maintaining the constant pre-selected rate of reduction throughout a large proportion of the main reduction step to Fe. The temperature then increases again toward the end of the reduction during the deceleration stage when nuclei begin to overlap and cause a decrease in the reaction interface.

Figure 8 shows α versus temperature plots obtained for the reduction of Fe_3O_4 starting material under linear heating rate (Figure 8a) and CRTA "rate-jump" (Figure 8b) conditions. The reduction is seen to occur in a single step and the shape of the CRTA plot again indicates that the reduction to metal proceeds via a nucleation or autocatalytic process.

Apparent activation energies were calculated from both linear heating rate and CRTA "rate-jump" profiles. Using the linear heating rate results shown in Table 2, a plot of $\ln(\beta/T_m^2)$ versus $1/T_m$ was found to be a straight line for both peaks associated with the reduction of Fe_2O_3 sample. Using the equations of these

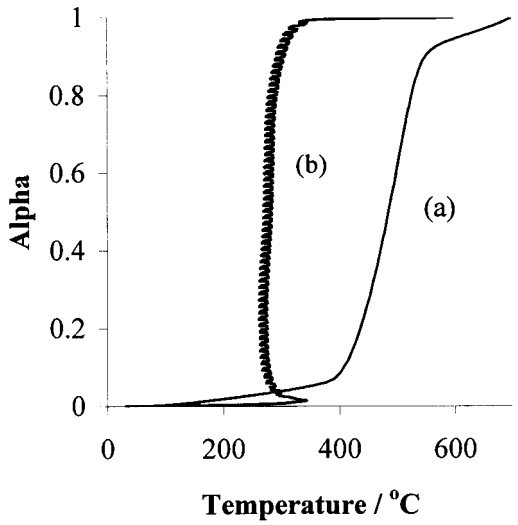

Figure 8. Extent of reaction (α) versus temperature plot for the TPR of Fe_3O_4 under (a) linear heating and (b) CRTA "rate-jump" conditions.

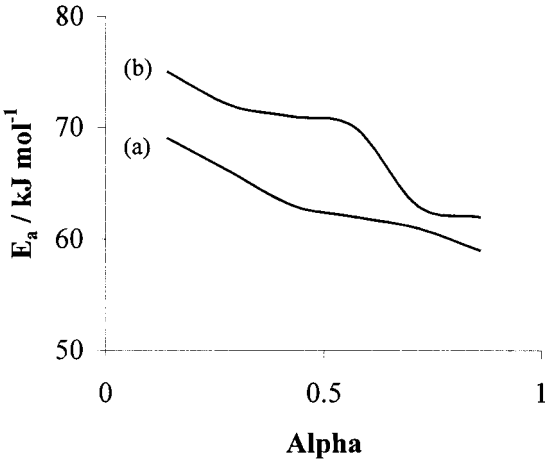

Figure 9. Apparent activation energy (E_a) for Fe_3O_4 reduction as a function of the extent of reduction (α), measured from CRTA "rate-jump" experiments for (a) Fe_3O_4 to Fe reduction step in the reduction of Fe_2O_3 starting material and (b) reduction of Fe_3O_4 starting material.

lines, the apparent activation energy for each step was calculated using eq 2. A value of 105.3 kJ mol^{-1} was calculated for the prereduction of Fe_2O_3 to Fe_3O_4 (equation of line; $Y = -12674.0X + 9.2$, correlation coefficient = 0.998) and a value of 53.6 kJ mol^{-1} was found for the main reduction step of Fe_3O_4 to Fe (equation of line; $Y = -6446.4X - 2.5$, correlation coefficient = 0.996).

In the same manner, the results in Table 3 were used to calculate the apparent activation energy for the reduction of the Fe_3O_4 sample to Fe. A plot of $\ln(\beta/T_m^2)$ versus $1/T_m$ was found to be a straight line described by the equation $Y = -7730.0X - 1.0$ (correlation coefficient = 0.998). Using eq 2, E_a was calculated to be 64.3 kJ mol^{-1}. The higher apparent activation energy, relative to that for the reduction of Fe_3O_4 formed from Fe_2O_3 starting material, may be associated with the different textural characteristics of the two starting materials.[2]

We have previously reported that the use of a CRTA "rate-jump" method to calculate apparent activation energies for metal oxide reduction can allow a more meaningful insight into variations of E_a throughout the reduction process when compared with linear heating rate methods.[18] As discussed above, the temperature profiles shown in Figures 5 and 6 show how the sample temperature was varied in order to alternate between the two pre-selected reaction rates throughout the reduction process(es) involved. E_a was calculated for each individual jump using eq 3. For the reduction of Fe_2O_3 to Fe_3O_4, E_a was found to be independent of α in that, while there was some scatter, there was no obvious trend recognized. The average value of E_a for this prereduction step was 96 kJ mol^{-1}. Although only a small number of "rate-jumps" were achieved for this step, an extrapolation technique[22] was used to help ensure that the temperature measurements, T_1 and T_2, for the target reduction rates, C_1 and C_2, were made at the same value of α for each jump. For the reduction of Fe_3O_4 to Fe, results showed that the apparent activation energy decreased over the course of the reduction as illustrated in Figure 9 which is consistent with an autocatalytic effect.[18] Similar results have been reported for the reduction of CuO where E_a has been found to decrease with extent of reduction under both isothermal[32,33] and CRTA "rate-jump" conditions.[18] The reduction of CuO is reported to follow a similar type of mechanism, involving formation and growth of nuclei or autocatalytic effects, to that presently found for the reduction of Fe_3O_4 and one possibility[18] is that lower values of E_a exist for the growth stage of the process relative to those required for the initial nucleation stage.

4.4. Comparison with Literature Kinetic Studies. In general, the reduction of Fe_3O_4, at lower temperatures and with smaller particle sizes, has been reported to show sigmoidal isothermal reduction curves characteristic of an induction period attributed to a nucleation process as the rate-determining step and involving uniform internal reduction.[1,8] With increasing particle size or reduction temperature, the literature indicates that this induction period becomes less pronounced with a shift in mechanism to one associated with a topochemical mode of reaction where chemical reaction at the oxide/Fe interface and/or diffusion through a porous Fe product layer (>7 mm particle sizes) becomes rate-determining.[1,8]

Table 4 summarizes the findings of the current and previous studies on the mechanism and activation energy of the reduction of powdered Fe_2O_3 and Fe_3O_4 samples. From this table, it is clear that even for the study of powdered samples, which would all be expected to have relatively small particle sizes, discrepancies do exist with respect to the mechanism of reduction reported. Wimmers et al.[1] studied the reduction of extremely small Fe_2O_3 particles (0.3 μm average diameter) under linear heating conditions. In dry H_2/Ar, step 2 of the reduction process occurred via a nucleation mechanism in agreement with that found in the current study. Evaluation of the mechanism of hematite to magnetite (step 1) was not possible due to a lack of resolution under the linear heating rate reduction conditions employed in the study.[1] In direct contrast to the findings of the current work, Shimokawabe et al.[2] reported that the $Fe_3O_4 \rightarrow$ Fe main reduction step was reported to proceed via a phase boundary mechanism while the prereduction step of $Fe_2O_3 \rightarrow Fe_3O_4$ involved formation and random growth of nuclei under isothermal conditions.[2] Sastri et al.[3] also reported a two-step mechanism via magnetite for the reduction of hematite under isothermal conditions and concluded that the overall rate of reaction was phase-boundary controlled with the topochemical reduction of Fe_3O_4 to Fe proceeding via formation and nucleation of metallic iron.

Table 4 also shows that discrepancies exist within the literature with regard to the measured activation energies for the reduction of powdered iron oxides. Such variations may be associated with differences between the samples studied and/or the conditions employed for sample pretreatment and/or reduction.[1−3] For example, Shimokawabe et al.[2] prepared

TABLE 4: Comparison of Kinetic Models and Activation Energies for the Reduction of Fe_2O_3 Found in This Work and in the Literature

source	reduction step	reduction mechanism	E (kJ mol^{-1})	method
Wimmers et al.[1]	$Fe_2O_3 \rightarrow Fe_3O_4$	n/d[c]	n/d[c]	linear heating rate
	$Fe_3O_4 \rightarrow Fe$	random nucleation	111	linear heating rate
Shimokawabe et al.[2]	$Fe_2O_3 \rightarrow Fe_3O_4$	random nucleation	74−117[a]	linear heating rate
	$Fe_3O_4 \rightarrow Fe$	phase boundary	60−73[a]	linear heating rate
Sastri et al.[3]	$Fe_2O_3 \rightarrow Fe$	phase boundary	57−73[a]	isothermal
this work	$Fe_2O_3 \rightarrow Fe_3O_4$	n/d[c]	106	linear heating rate
	$Fe_3O_4 \rightarrow Fe$	n/d[c]	54	linear heating rate
this work	$Fe_2O_3 \rightarrow Fe_3O_4$	phase boundary	96	CRTA "rate-jump"
	$Fe_3O_4 \rightarrow Fe$	random nucleation	59−69[b]	CRTA "rate-jump"

[a] depending on heating conditions employed for pretreatment prior to reduction. [b] depending on the extent of reduction. [c] n/d − not determined.

α-Fe_2O_3 by the decomposition of iron salts in air at temperatures of between 500 °C and 1200 °C and found that samples prepared by decomposition at higher temperatures had greater activation energies for the reduction than those prepared at lower temperatures. This was associated with a higher reactivity of smaller particles for samples prepared at lower temperatures and was more particularly pronounced for the prereduction step of Fe_2O_3 to Fe_3O_4 than for the main reduction to Fe. Sastri et al.[3] reported that pretreatment at 850 °C of α-Fe_2O_3 resulted in an increase in activation energy to 73 kJ mol^{-1} relative to a value of 57 kJ mol^{-1} for a sample that had undergone no heat treatment. Thus, E_a is strongly sample dependent.

In the present study differences, albeit fairly small, exist (see Table 4) between the activation energies measured under linear heating rate conditions relative to those obtained using the CRTA "rate-jump" method. Of course, the latter technique also reveals changes in the energy of activation throughout the reduction of Fe_3O_4 to Fe (see Figure 9). Use of the CRTA "rate-jump" method for the measurement of E_a values for solid-state reactions has been recommended because heat and mass transfer effects are minimized[18,26,29] while the ability to completely resolve individual processes ensures that the values obtained are strictly associated with a given process. Hence, it is contended that the values obtained using this method (rather than linear heating rate experiments) more closely approximate to the true activation energy for the reduction of the iron oxide powders studied. This is particularly so for the Fe_3O_4 to Fe reduction whereas measurement of E_a under CRTA "rate-jump" conditions for the prereduction of Fe_2O_3 to Fe_3O_4 may be slightly less accurate due to the smaller number of jumps achieved.

It must be stressed that the apparent activation energy of thermal processes is sample-dependent and affected by factors such as grain size, crystallinity, purity, and the thermal history of the material under study.

Conclusions

The reduction of both Fe_2O_3 and Fe_3O_4 samples to Fe were studied under linear heating rate and CRTA "rate-jump" conditions. The latter technique resulted in improved resolution of overlapping reduction events and allowed a detailed insight to be gained into the apparent activation energies and mechanisms involved in each event.

The reduction of Fe_2O_3 was found to occur in a two-step process via Fe_3O_4. CRTA experiments showed that the two steps occurred consecutively. The shape of the CRTA profile indicated that the prereduction step (Fe_2O_3 to Fe_3O_4) was described by an "*n*th-order" expression where nucleation or diffusion were not the rate-controlling process. The reduction of Fe_3O_4 thus formed to metallic iron followed a nucleation/autocatalytic mechanism. The CRTA profile obtained for the reduction of Fe_3O_4 starting material to Fe also showed this reduction process to involve nucleation and/or autocatalysis.

CRTA "rate-jump" profiles allowed the measurement of apparent activation energies as a function of the extent of reaction for the different reduction processes. For the reduction of Fe_2O_3, E_a was found to be 96 kJ mol^{-1} for the initial reduction to Fe_3O_4. For the main reduction step to Fe, E_a decreased from 69 to 59 kJ mol^{-1} as the reduction proceeded. Similarly, for the reduction of Fe_3O_4 starting material, E_a decreased from 75 to 61 kJ mol^{-1} as the reaction progressed from start to finish. The differences between these two sets of values is thought to reflect the effects of sample morphology in the apparent activation energy of the reduction process.

It should be noted that the kinetics of the reduction reactions are expected to be strongly sample-dependent and further studies, using the advantages of the CRTA "rate-jump" method may elucidate the effects of parameters such as particle size and the presence of various impurities or promoters in the iron oxide phase on the reduction processes.

Acknowledgment. The authors gratefully acknowledge the generous support of the Engineering and Physical Sciences Research Council (EPSRC) in funding this program of work (Grant No. GR/L19539).

References and Notes

(1) Wimmers, O. J.; Arnoldy P.; Moulijn, J. A. *J. Phys. Chem.* **1986**, *90*, 1331.
(2) Shimokawabe, M.; Furuichi, R.; Ishii, T. *Thermochim. Acta* **1979**, *28*, 287.
(3) Sastri, M. V. C.; Viswanath R. P.; Viswanath B. *Int. J. Hydrogen Energy* **1982**, *7*, 951.
(4) Viswanath, R. P.; Viswanath B.; Sastri, M. V. C. *React. Kinet. Catal. Lett.* **1975**, *2*, 51.
(5) Jung H.; Thompson, W. J. *J. Catal.* **1991**, *128*, 218.
(6) Boot, L. A.; van Dillen, A. J.; Geus J. W.; van Buren, F. R. *J. Catal.* **1996**, *163*, 186.
(7) van Ommen, J. G.; Bosch, H.; Gellings. P. J.; Ross, J. R. H. In *Studies in Surface Science and Catalysis*; Delmon, B., Grange, P., Jacobs, P. A., Poncelet, G., Eds.; Elsevier: Amsterdam, 1987; Vol. 31, p 151.
(8) Turkdogan E. T.; Vinters, J. V. *Metall. Trans.* **1972**, *3*, 1561.
(9) Edstrom, J. O. *J. Iron Steel Inst.* **1953**, *175*, 289.
(10) Quets, J. M.; Wadsworth M. E.; Lewis, J. R. *Trans. Metall. Soc. AIME* **1960**, *218*, 545.
(11) Somorjai, G. A. *Surface Chemistry and Catalysis*; Wiley-Interscience: New York, 1994; Chapter 7.
(12) Hurst, N. W.; Gentry, S. J.; Jones, A.; McNicol, B. D. *Catal. Rev.—Sci. Eng.* **1982**, *24* (2), 233.
(13) Ortega, A. *Thermochim. Acta* **1996**, *284*, 379.
(14) Cioci, F.; Lavecchia, R.; Fierro, G.; Lo Jacono, M.; Inversi, M. *Thermochim. Acta* **1996**, *287*, 351.
(15) Malet, P.; Caballero, A. *J. Chem. Soc., Faraday Trans. 1* **1988**, *84* (7), 2369.
(16) Stuchly, V. *J. Therm. Anal.* **1989**, *35*, 837.
(17) Monti, D. A.; Baiker A. *J. Catal.* **1983**, *83*, 323.
(18) Tiernan, M. J.; Barnes, P. A.; Parkes, G. M. B. *J. Phys. Chem.* **1999**, *103*, 338.
(19) Barnes, P. A.; Parkes, G. M. B.; Brown, D. R.; Charsley, E. L. *Thermochim. Acta* **1995**, *269/270*, 665.

(20) Rouquerol, J. *Thermochim. Acta* **1989**, *144*, 209.
(21) Ortega, A.; Akhouayri, S.; Rouquerol, F.; Rouquerol, J. *Thermochim. Acta* **1994**, *235*, 197.
(22) Tiernan, M. J.; Barnes, P. A.; Parkes, G. M. B. *J. Phys. Chem.* **1999**, *103*, 6944.
(23) Sharp, J. H.; Brindley, G. W.; Narahari Acker, B. M. *J. Am. Chem. Soc.* **1966**, *49*, 379.
(24) Criado, J. M.; Ortega, A.; Gotor, F. J. *Thermochim. Acta* **1990**, *157*, 171.
(25) Malek, J.; Sestak, J.; Rouquerol, F.; Rouquerol, J.; Criado, J. M.; Ortega A. *J. Therm. Anal.* **1992**, *38*, 71.
(26) Reading, M.; Dollimore, D.; Rouquerol, F.; Rouquerol, J. *J. Therm. Anal.* **1984**, *29*, 775.
(27) Maciejewski, M. *J. Therm. Anal.* **1992**, *38*, 51.
(28) Parkes, G. M. B.; Barnes, P. A.; Charsley, E. L. *Thermochim. Acta* **1998**, *320* (1−2), 297.
(29) Reading, M.; Dollimore, D.; Whitehead, R. *J. Therm. Anal.* **1991**, *37*, 2165.
(30) Baldi, M.; Escribano, V. S.; Amores, J. M. G.; Milella, F.; Busca, G. *Appl. Catal. B* **1998**, *17*, L175.
(31) Barnes, P. A.; Tiernan, M. J.; Parkes, G. M. B. *J. Therm. Anal. Calorim.* **1999**, *56*, 733.
(32) Voge, H. H.; Atkins, L. T. *J. Catal.* **1962**, *1*, 171.
(33) Hayden, B. E.; Lamont, C. L. A. *J. Phys. Condens. Matter* **1989**, *1*, SB33.